Supporting Information

Schiffer et al. 10.1073/pnas.1006614107

SI Methods

Genital Swabbing Protocols. Herpes simplex virus (HSV) serologic testing was performed by Western blot to confirm HSV-2 infection in each study subject (1). We analyzed 1,736 shedding episodes from 632 participants enrolled in 17 protocols involving daily home collection of genital swabs between 1990 and 2008. Participants did not take antiviral medicines to suppress herpes and were not HIV-1 infected. To avoid overrepresentation, we kept only the first 10 episodes per participant. We deleted 707 episodes of uncertain duration, leaving 1,003 shedding episodes from 386 persons. No subjects were within 1 y of HSV acquisition; 155 (40%) participants were men; 320 (90%) were white, 21 (6%) black, and the remaining 4% either Asian or mixed. One hundred sixty-nine (44%) were HSV1 coinfected. Each contributed at least 30 d of swabs (median = 55, range = 30–325).

Genital Swabs and PCR for HSV-2 DNA. Genital swabs were placed into vials containing 1 mL of PCR transport medium and refrigerated until laboratory processing (2). HSV DNA was detected by using a quantitative PCR assay, and the HSV DNA level was expressed as copies per milliliter of transport medium (3). The initial PCR assay used type-common primers to the HSV gene encoding glycoprotein B. Positive samples were subsequently analyzed by using type-specific primers to examine whether the DNA detected was HSV-1, HSV-2, or both (4). An internal control was included to ensure that HSV-negative swabs were not due to inhibition. Laboratory personnel were blinded to clinical data.

Mucosal Immune Response in Study Participants. We defined the spatiotemporal dynamics of HSV-2–specific lymphocyte response to a genital recurrence by using in situ staining of genital skin biopsy with HSV-2 antigen-specific quantum dot multimers. We then examined the biopsy specimens with confocal microscopy, which revealed that several weeks after lesion healing, dendritic cells and $CD4^+$ lymphocytes congregate in the perivascular space in postcapillary venule tufts in the rete ridges of the upper dermis. $CD8^+$ lymphocytes appeared at the precise site of HSV release from the neuron termini, the dermal/epidermal junction, and in the contiguous dermis and epidermis. Based on staining results, we enumerated $CD8^+$ T cells before, during, and 2, 4, 6, and 8 wk after an HSV-2 recurrence (5, 6).

Previous studies indicated that at least 10% of $CD8^+$ T cells detected in tissue at the dermal–epidermal junction are HSV-2–specific and that this proportion remains constant as $CD8^+$ T-cell levels fluctuate. Approximately 90% of $CD8^+$-selected lymphocytes after expansion with a chromium release assay are $CD3^+$/$CD8^+$, whereas 3% are $CD8^+/CD3^-/CD56^+$ NK cells, indicating that the majority of $CD8^+$ cells are cytolytic T cells (5). As such, we used data derived from in situ staining of $CD8^+$ T cells to define relative densities of HSV-2–specific $CD8^+$ T cells in mucosal tissue.

In prior studies, the absolute number of $CD8^+$ lymphocytes was measured per mm^2 of genital skin (5, 6). These measures are likely to be underestimates for the total number of $CD8^+$ T cells present in the entire lesion area. First, most lesions are larger than 1 mm^2. Second, $CD8^+$ lymphocyte density was highest at the lesion edge, whereas $CD8^+$ T cells were present in 25-fold lower densities 2 to 5 cm away from the lesion edge. $CD8^+$ T-cell density presumably decreases according to a gradient across this 2-cm distance. However, biopsies were not performed within the 2-cm radius from the lesion, and $CD8^+$ T cells 0–2 cm away from the lesion edge were not counted. Finally, the biopsy studies enumerated $CD8^+$ T cells from cross-sectional biopsies in two dimensions only. Despite these facts, the values of sequential $CD8^+$ T-cell densities gathered every 2 wk accurately measured the "relative" intensity of the immune response at different points in time. These relative measures were adequate to recreate model dynamics of $CD8^+$ replenishment and decay (7).

Mathematical Model of HSV-2 Episode Clearance. The model's ordinary differential equations described infection of susceptible epithelial cells (S), release of virus (Y) from infected neurons, release of virus (Z) from infected epithelial cells (I), and clearance of infected cells by $CD8^+$ lymphocytes (E), which replenished in number in response to infected cells and decay at a fixed exponential rate. We also included a variable (V) for total virus ($Z + Y$), which we used to fit model output to the quantitative PCR data from genital swabs. The stochastic model equations were updated at a time step of 0.001 d by randomly selecting integer values from binomial distribution functions for nonlinear model terms and poisson distributions for linear terms. We performed most simulations by using Berkeley Madonna, Version 8.3.18 (Macey and Oster), and performed our 10,000 serial simulations (Table S2) with C++.

We described virologic model output according to several standard clinical definitions. In this article, we used the term "reactivation" to describe a shedding episode that was detectable by using PCR or culture from a genital swab, rather than to describe release of virus from the neural ganglia. In the literature, both definitions are often used. However, in a prior published manuscript based on the mathematical model, we predicted that not all of the viral particles that arrive via neuron endings into genital tract skin infect epidermal cells, and that replication of HSV within epidermal cells, rather than release from neurons, leads to detection of virus with a genital swab. In addition, the model output suggested that neuronal release of HSV may occur almost constantly, whereas episode initiation occurs sporadically when a single epidermal cell became infected (7). We assume in this manuscript that reactivation describes the latter phenomenon.

An HSV-2 reactivation that results in mucosal HSV shedding can be subclinical or clinical. Clinical shedding is termed a "recurrence" and is associated with sporadic crops of vesicles and/or erosions, which form because of a large plaque of closely congregated, dead epithelial cells. A group of closely approximated vesicles and/or ulcers is termed a "lesion" (8). "Subclinical shedding episodes" are common during chronic HSV-2 infection and are defined by local detection of virus either by viral culture or PCR in the absence of a clinically apparent genital lesion or symptoms (9, 10). Subclinical episodes are also typically associated with a lower copy number of HSV and more rapid clearance from the genital tract (11). The model captures both types of episodes and attributes subclinical episodes to fewer infected cells before lesion clearance (7).

Model terms were defined according to stage of infection and were driven by several model parameters, which we maintained at constant values throughout simulations unless otherwise noted. Estimates for realistic parameter value ranges were derived from published and experimental data (5, 12–19). During the "latent phase" of genital HSV infection, virus is maintained in a dormant state in the sacral ganglia. HSV-2 virions (variable Y in the model) are periodically released from neuronal endings at the dermal–epidermal junction at a certain rate (ϕ). This parameter represented its own birth term in the model. Released virions survive within cell junctions in the genital tract for a defined duration ($1/c$) during which time they can infect local epithelial cells. The death term for virions produced by neurons in our model was ($c \times Y$), whereas the disappearance of viruses due to infection of a cell

was described by the term ($\beta \times S \times Y$). Similarly, the death term for virions produced by epidermal cells was ($c \times Z$), whereas the disappearance of this set of viruses due to infection of a cell was described by the term ($\beta \times S \times Z$).

Viral infectivity ($1/(\beta \times S_0)$), where S_0 is the initial number of susceptible cells, was defined as the number of viruses that are needed to infect an average of one epithelial cell per day assuming constant presence of viruses and susceptible cells. If an epithelial cell converted from susceptible to infected because of viral entry into the cell (term = $\beta \times S \times V$), then we assumed that it would die either via direct viral lysis if the cell survived long enough to become packed with viruses and lose its function (lifespan = $1/a$), or it would die via $CD8^+$ lymphocyte-mediated killing [lifespan = $1/(a + (f \times E))$]. Lymphocyte killing efficiency (f) was defined as the number of infected cells cleared by one $CD8^+$ lymphocyte cell (among a population of infiltrating $CD8^+$ T cells) per day in vivo. The death terms for infected cells from lysis and $CD8^+$-mediated killing were ($a \times$ I) and ($f \times I \times E$), respectively.

If an epithelial cell evaded $CD8^+$ lymphocyte-mediated killing for the entire duration of cellular infection, it produced a total of p/a viruses: This number represented the burst phase of each infected cell; p was defined as the rate of viruses produced by an infected cell per day. $p/(a + (f \times T))$ was the per cell average viral production at any point in time.

The model accounted for the fact that clearance of a clinically apparent genital lesion is associated with a rapid accumulation of $CD8^+$ T lymphocytes into the lesion area. We assumed accumulation of $CD8^+$ T lymphocytes into the lesion area at a peak rate (θ), with birth term ($\theta \times E \times (I/(I + r))$), where r was the number of infected cells needed before half-maximal rate of $CD8^+$ T-cell expansion rate. Parameter r at least indirectly captured the effectiveness of antigen uptake and presentation, costimulation of T cells by antigen-presenting cells, and $CD8^+$ T-cell activation by other immune signaling pathways. This infiltration of $CD8^+$ T cells is then associated with a slow decay of these cells over a period of months after lesion healing [lifespan = $1/\delta$, death term ($E \times \delta$)] (5).

The small diameter of genital lesions in the immunocompetent host, despite the presence of nearly infinite numbers of target cells (all skin cells are competent for replication and spread of HSV), allowed for the assumption that target cells are not limited during HSV infection. Therefore, the mathematical definition of the reproductive number (R_0), which assumed no immunity, also assumed no target cell limitation. Without T-cell pressure, an infected cell produced p/a virions and each virus survived for $1/c$ days. Therefore, during a cell's complete cycle of infectiousness, the cell harbored an average of $p/(a \times c)$ viruses that could infect adjacent cells. Assuming no target limitation, $\beta \times S_0$ represented the rate of infectivity of a single virus per day. Therefore, the total number of cells infected by the p/a virions produced by a single cell was $(p \times \beta \times S_0)/(a \times c)$ or R_0, where S was only a small fraction less than S_0 during the entire course of an episode.

The reproductive number (R) was derived by using the same method as R_0 for the model but was inclusive of immunologic response. Hence, the lifespan of the infected cell was influenced by the presence of cytolytic $CD8^+$ T cells and was $1/(a + (f \times T))$. Therefore, $R = (p \times \beta \times S_0)/((a + fT) \times c)$ and varies according to lymphocyte density. Given the highly stochastic nature of viral spread and immune clearance during the early stages of a shedding episode, it is worth emphasizing that R was an average value for all infected cells.

Model Fitting to Patient Data and Stochastic Simulations. In a prior study, we estimated parameter values by fitting a determinstic version of the model to 89 virologic curves generated from serial quantitative anogenital HSV-2 PCR swabs in patients with clinically, serologically, and virologically documented recurrent HSV-2 infection who developed a genital lesion. The data were obtained from studies of the natural history of genital HSV-2 in which quantitative HSV PCR was collected on a daily basis from patients (9, 10, 20). We used least squares regression analysis to fit the model to each individual viral curve. We could not entirely rule out the possibility of local minima based on a relatively high number of unsolved parameters. However, for each of the 89 model fits, we were able to produce realistic model output.

Once parameters were estimated for each of the 89 episodes, we converted the model to a stochastic stage-structured form with otherwise unchanged compartmental structure (7, 21). For the fixed parameter set in the current paper, we selected approximate median values of parameters obtained in the past analysis because these parameter values typically generated realistic proportions of low-, medium-, and high-copy episodes during stochastic simulations. We rounded parameter values within the fixed parameter set for simplicity. We also used 20 randomly selected parameter sets from the original 89 curves for further simulations. Finally, we performed a sensitivity analyses in which we adjusted each of the parameter values to values 20% below and above the median values.

Lesion Diameter Estimates. We estimated the number of susceptible cells before introduction of virus (S_0) based on the number of cells that pack into a hypothetical 2-cm–diameter cylinder with volume equal to height multiplied by area of a circle. We examined skin biopsies of genital lesions to define the average depth between the peripheral nerve endings and the outermost layer of nucleated, susceptible epithelial cells. To estimate the radius of a single cell on digitized histology slides, we used Free Ruler 1.7b5 (www.pascal.com) to measure the diameter of the ten largest "stratum spinosum" cells from a 400-μm-wide biopsy of the perianal skin, averaged these measurements, and divided the mean by two (cell radius = 8.5 μm). To estimate the height of the cylinder of susceptible cells in a 2-cm–diameter area of anogenital skin, and to account for the uneven nature of the dermal/epidermal borders, we took 20 evenly spaced vertical measurements from the dermal/epidermal junction to the bottom of the "stratum lucidum" and then calculated the mean of these numbers. These height measurements were then performed individually on several perianal skin histology slides and averaged (74 μm). Similar numbers of cells were predicted whether we assumed cuboidal (4.7318*e*6) or spheroid cell shape (5.4223*e*6). We chose spheroid cell shape for all runs of the model. Calculations are all performed with units of millimeters.

Assuming Spheroidal Cell Shape. Initial number of susceptible cells (stratum spinosum/basale/granulosum) = (Volume of susceptible area in genital mucosa/Volume of a spheroid cell) × adjustment factor for how many spheres fit into a column = ((height × π × radius^2)/(4/3 × π × cell radius^3)) × 0.6 = ((74 × π × 10,000^2)/(4/3 × π × 8.5^3)) × 0.6 = 5.4223*e*6.

Assuming Cuboidal Cell Shape. Volume of susceptible area in genital mucosa/Volume of a cuboidal cell = (height × π × radius^2)/(8 × cell radius^3) = (74 × π × 10,000^2)/(8 × 8.5^3) = 4.7318*e*6.

Calculation of Lesion Diameter. We calculated lesion diameter by subtracting the number of susceptible and infected cells at a certain point in time from the initial number of susceptible cells. The difference in this equation is the number of cells that have been infected and died, but have yet to grow back according to the logistic growth function:

Number of missing cells = 5.4223*e*6 (i.e., total number of cells) $- S - I$ = Ulcer area/Volume of a cell = $(74 \times \pi \times (R \wedge 2) \times 0.64)/(4/3 \times \pi \times 8.5^3)$ where R = radius of an ulcer.

$$5.4223e6 - S - I = (74 \times \Pi \times (R\wedge 2) \times 0.64)/(4/3 \times \Pi \times 8.5^3)$$

Diameter of an ulcer = $R \times 2$.

Therefore, diameter of an ulcer = $2 \times \sqrt{(9.38123e7 - (S + I)/0.0578)}$

We defined a recurrence as lesion of >2 mm in diameter.

1. Ashley RL, Militoni J, Lee F, Nahmias A, Corey L (1988) Comparison of Western blot (immunoblot) and glycoprotein G-specific immunodot enzyme assay for detecting antibodies to herpes simplex virus types 1 and 2 in human sera. *J Clin Microbiol* 26: 662–667.
2. Jerome KR, Huang ML, Wald A, Selke S, Corey L (2002) Quantitative stability of DNA after extended storage of clinical specimens as determined by real-time PCR. *J Clin Microbiol* 40:2609–2611.
3. Magaret AS, Wald A, Huang ML, Selke S, Corey L (2007) Optimizing PCR positivity criterion for detection of herpes simplex virus DNA on skin and mucosa. *J Clin Microbiol* 45:1618–1620.
4. Corey L, Huang ML, Selke S, Wald A (2005) Differentiation of herpes simplex virus types 1 and 2 in clinical samples by a real-time taqman PCR assay. *J Med Virol* 76: 350–355.
5. Zhu J, et al. (2007) Virus-specific CD8$^+$ T cells accumulate near sensory nerve endings in genital skin during subclinical HSV-2 reactivation. *J Exp Med* 204:595–603.
6. Zhu J, et al. (2009) Persistence of HIV-1 receptor-positive cells after HSV-2 reactivation is a potential mechanism for increased HIV-1 acquisition. *Nat Med* 15: 886–892.
7. Schiffer JT, et al. (2009) Frequent release of low amounts of herpes simplex virus from neurons: Results of a mathematical model. *Sci Transl Med* 1:7ra16.
8. Corey L, Adams HG, Brown ZA, Holmes KK (1983) Genital herpes simplex virus infections: Clinical manifestations, course, and complications. *Ann Intern Med* 98: 958–972.
9. Wald A, et al. (2000) Reactivation of genital herpes simplex virus type 2 infection in asymptomatic seropositive persons. *N Engl J Med* 342:844–850.
10. Wald A, Zeh J, Selke S, Ashley RL, Corey L (1995) Virologic characteristics of subclinical and symptomatic genital herpes infections. *N Engl J Med* 333:770–775.
11. Mark KE, et al. (2008) Rapidly cleared episodes of herpes simplex virus reactivation in immunocompetent adults. *J Infect Dis* 198:1141–1149.
12. Ganusov VV, De Boer RJ (2008) Estimating in vivo death rates of targets due to CD8 T-cell-mediated killing. *J Virol* 82:11749–11757.
13. De Boer RJ, Homann D, Perelson AS (2003) Different dynamics of CD4+ and CD8$^+$ T cell responses during and after acute lymphocytic choriomeningitis virus infection. *J Immunol* 171:3928–3935.
14. Regoes RR, Yates A, Antia R (2007) Mathematical models of cytotoxic T-lymphocyte killing. *Immunol Cell Biol* 85:274–279.
15. Regoes RR, Barber DL, Ahmed R, Antia R (2007) Estimation of the rate of killing by cytotoxic T lymphocytes in vivo. *Proc Natl Acad Sci USA* 104:1599–1603.
16. Barchet W, et al. (2000) Direct quantitation of rapid elimination of viral antigen-positive lymphocytes by antiviral CD8(+) T cells in vivo. *Eur J Immunol* 30:1356–1363.
17. Turner R, Shehab Z, Osborne K, Hendley JO (1982) Shedding and survival of herpes simplex virus from 'fever blisters'. *Pediatrics* 70:547–549.
18. Jiang C, et al. (2007) Herpes simplex virus mutants with multiple substitutions affecting DNA binding of UL42 are impaired for viral replication and DNA synthesis. *J Virol* 81:12077–12079.
19. Jiang C, Hwang YT, Randell JC, Coen DM, Hwang CB (2007) Mutations that decrease DNA binding of the processivity factor of the herpes simplex virus DNA polymerase reduce viral yield, alter the kinetics of viral DNA replication, and decrease the fidelity of DNA replication. *J Virol* 81:3495–3502.
20. Brock BV, Selke S, Benedetti J, Douglas JM, Jr., Corey L (1990) Frequency of asymptomatic shedding of herpes simplex virus in women with genital herpes. *JAMA* 263: 418–420.
21. Chao DL, Davenport MP, Forrest S, Perelson AS (2004) A stochastic model of cytotoxic T cell responses. *J Theor Biol* 228:227–240.

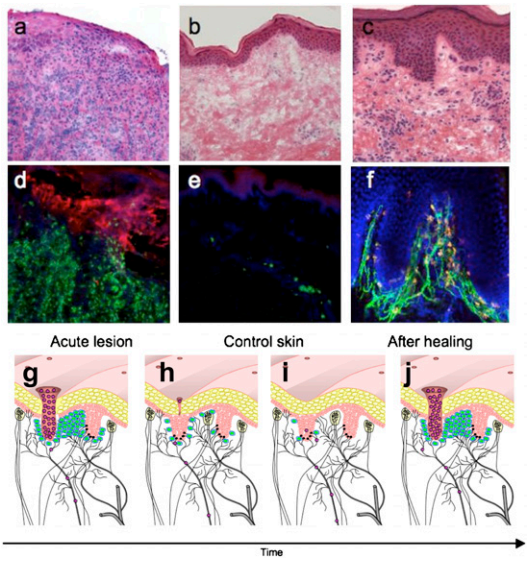

Fig. S1. Local CD8$^+$ responses during and after a genital herpes recurrence. Hematoxylin and eosin staining of lesional (*A*) and normal control (*B*) skin during genital HSV-2 reactivation, and of healed skin 8 wk after complete resolution of herpes (*C*). Immunofluorescent staining for CD8$^+$ T cells (green) and HSV-2–infected cells (red) in lesion (*D*) and normal (*E*) skin. (*F*) CD8$^+$ T cells (orange) persisted and accumulated near peripheral nerve endings (NCAM$^+$, green) at the dermal-epidermal junction of a lesion site 12 wk after complete healing; cartoon display of CD8$^+$ lymphocyte response to HSV-2 shedding in the genital skin. CD8$^+$ lymphocytes accumulate at the dermal epidermal junction in high numbers during a genital lesion (*G*), decay slowly and persist in the setting of low-copy shedding and continual release of HSV-2 from peripheral neurons (*H*), persist for at least 4 mo after a lesion (*I*), and replenish in large numbers in response to further lesions at the reactivation site (*J*).

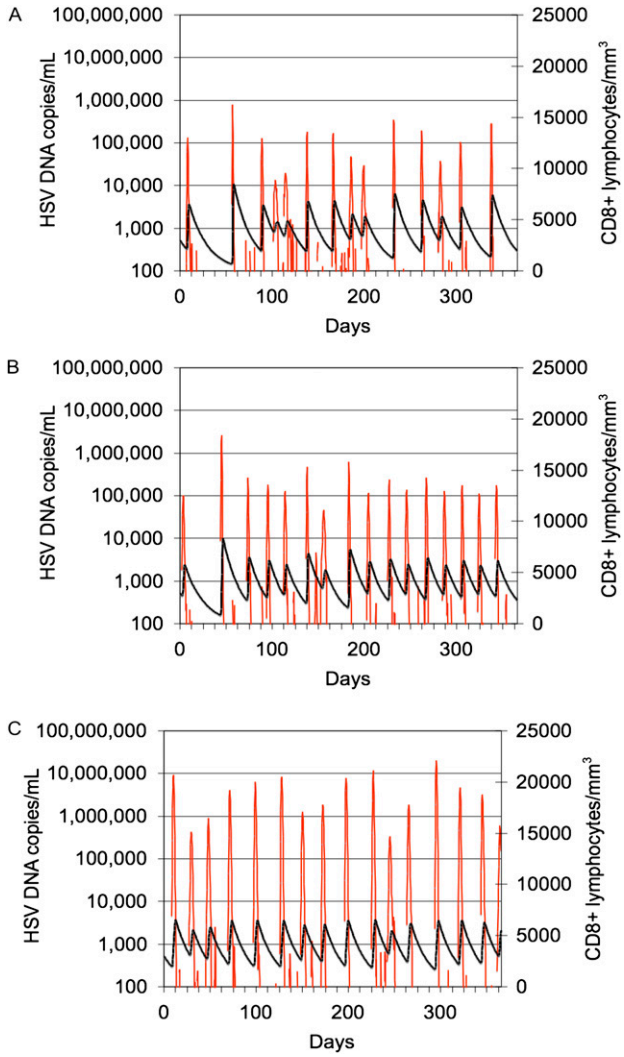

Fig. S2. Model simulations with model from Table S6. Distribution of episodes with peak copy number $>10^4$ HSV DNA copy number per milliliter showed less heterogeneity than distributions of episodes generated from model in Table S1. The peak copy number of episodes was determined by the $CD8^+$ T-cell infusion rate. (*A*) θ_I = 10,000/d. (*B*) θ_I = 6,000/d. (*C*) θ_I = 2,000/d.

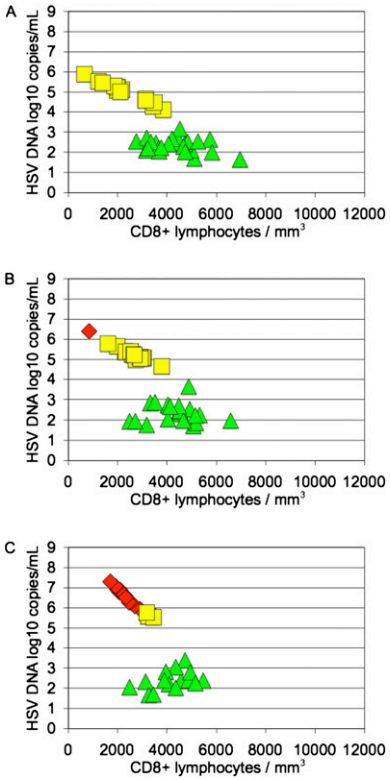

Fig. S3. In a 365-d model simulation, $CD8^+$ lymphocyte density (per mm^3) was inversely correlated with shedding episode peak HSV DNA copy number, even when $CD8^+$ lymphocyte trafficking from external sources, rather than local replication, was assumed (Table S6). Green triangles are low (10^2 to 10^4 peak HSV DNA copies per milliliter), yellow squares are medium ($<10^4$ to 10^6 peak HSV DNA copies per milliliter), and red diamonds are high-copy episodes ($>10^6$ peak HSV DNA copies per milliliter); HSV-2 DNA peak copy number per episode (*y* axis) and $CD8^+$ lymphocyte density at episode onset (*x* axis) shedding episodes from the 365-d simulations in Fig. S2*A* (*A*), Fig. S2*B* (*B*), and Fig. S2*C* (*C*).

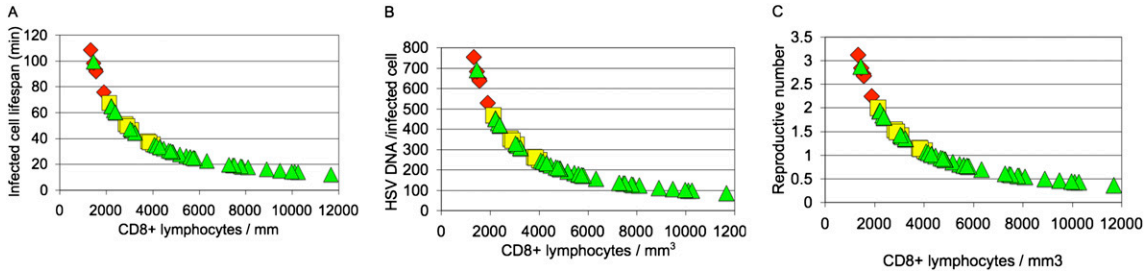

Fig. S4. $CD8^+$ lymphocyte density (per mm^3) in genital skin determines mean infected cell lifespan, mean viral production per infected cell, and reproductive number at episode onset. (*A*) Mean infected cell lifespan (*y* axis) and $CD8^+$ lymphocyte density (*x* axis) at episode onset. (*B*) HSV-2 production per infected cell (*y* axis) and $CD8^+$ lymphocyte density (*x* axis) at episode onset. (*C*) Reproductive number at episode onset (*y* axis) and $CD8^+$ lymphocyte density (*x* axis) at episode onset.

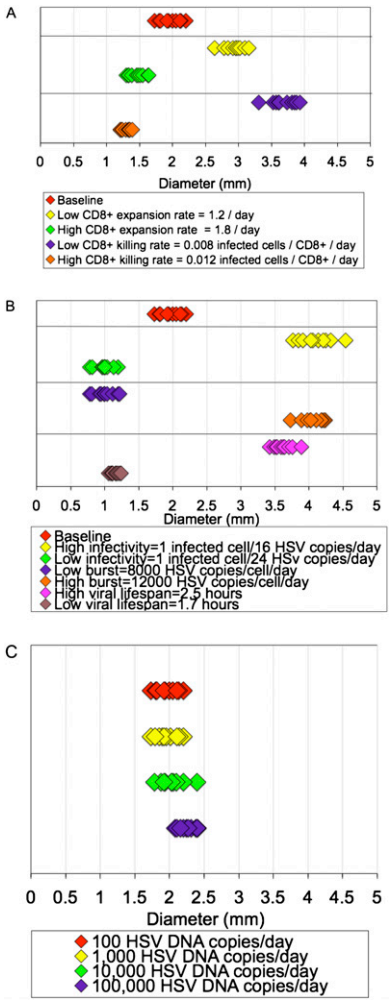

Fig. S5. Lesion diameter is closely related to host and viral events in the skin and mucosa. To isolate the effect of abrupt parameter value adjustments on shedding episode severity, shedding episodes were simulated at a low initial $CD8^+$ lymphocyte level ($\approx$1,700/mm^3). Ten shedding episode simulations were performed with baseline parameter values from Table 1 and neuronal release rate (ϕ) = 100 HSV DNA copies per day. Ten simulations were performed for each parameter set with an adjusted parameter value. (*A*) A 20% decrease in $CD8^+$ expansion rate, and $CD8^+$ killing rate resulted in substantially larger genital lesions. (*B*) A 20% increase in infectivity, infected cell burst phase, and viral lifespan resulted in substantially larger genital lesions. (*C*) A thousandfold increase in ϕ before episode initiation had little effect on lesion diameter.

Table S1. Stochastic mathematical models of HSV-2 pathogenesis: Model equations and mathematical model assumptions

Stochastic model equations	Variables (starting values)	Parameters (values)	Model assumptions
• $\Delta S = (\lambda - (\beta \times S \times V))\ \Delta t$	• S = susceptible epidermal cells (5.42e6)	• β = infectivity (10^{-8}/d)	• Viruses are created by neurons and epidermal cells; viruses are produced with different kinetics by neurons and epidermal cells; viruses infect epidermal cells at a constant per virus rate.
• $\Delta I = ((\beta \times S \times V) - (a \times I) - (f \times I \times E))\ \Delta t$	• I = infected epidermal cells (zero)	• a = infected cell death rate (1.2/d)	• Infected cells differ from susceptible epidermal cells in that they die more rapidly, produce viruses at a constant rate, and are susceptible to lysis by $CD8^+$ T cells.
• $\Delta E = ((f(I) \times \theta \times E) - \delta \times E))\ \Delta t$	• E = $CD8^+$ lymphocytes (6,000, average value from a prior 365-d simulation)	• f = $CD8^+$ T-cell killing rate (0.01 cells per $CD8^+$ T cell day)	• $CD8^+$ T cells are activated by the presence of infected cells, and in an activated state can replicate and lyse infected cells.
• $f(I) = I/(I+r)$	• Z = HSV DNA copy produced by an epidermal cell (zero)	• θ = $CD8^+$ T-cell expansion rate (1.5/d)	• $CD8^+$ T cells persist in the genital skin and decay at a fixed exponential rate.
• $\Delta Z = ((p \times I) - (c \times Z) - (\beta \times S \times Z))\ \Delta t$		• δ = $CD8^+$ T-cell decay rate (0.05/d)	• Viruses decay at a fixed rate.
• $\Delta Y = [\phi - (c \times Y) - (\beta \times S \times Y))\ \Delta t$		• r = no. of infected cells before half-maximal $CD8^+$ T-cell expansion rate (200 infected cells)	• Epidermal cells regenerate after dying but reach a carrying capacity at which point regrowth ceases.
• $\lambda = d(S_0 - S)$		• p = HSV DNA copies produced per day per epidermal cell (10,000 HSV DNA copies per epidermal cell per day)	
• $V = Z + Y$		• c = HSV virion decay rate (12/d)	
• Δt = 1.5 min		• ϕ = HSV DNA release rate per day from neurons (50 HSV DNA copies per day)	
		• d = logisitical epidermal regrowth parameter (0.22/d)	

Table S2. Episode characteristics from 10,000, 365-d model simulations assuming both continuous and daily sampling: Episode and shedding frequency of means, 95% confidence intervals, and ranges from 10,000 simulations

		Annual episodes for daily sampling				Annual episodes for continuous sampling			
Measures	Shedding frequency	High	Medium	Low	Total	High	Medium	Low	Total
Mean	17.1	3.3	9.4	7.1	19.8	4.1	8.7	54.3	67.1
95% CI	(17.0,17.2)	(3.3, 3.3)	(9.3, 9.4)	(7.1, 7.2)	(19.7, 19.9)	(4.1, 4.1)	(8.6, 8.7)	(54.1, 54.5)	(66.9, 67.2)
Range	(8.5, 36.2)	(0, 8)	(1, 19)	(0, 19)	(11, 33)	(0,8)	(1, 18)	(22, 101)	(33, 114)

Low-, medium-, and high-copy episodes are defined as having a peak HSV-2 DNA copy number 10^2–10^4/mL, 10^4–10^6/mL, and $>10^6$/mL, respectively.

Table S3. Episode characteristics from 10,000, 365-d model simulations assuming both continuous and daily sampling: $CD8^+$ T-cell density per mm^3 and average infected lifespan at episode onset of means, 95% confidence intervals, and ranges from 10,000 simulations

	$CD8^+$ lymphocytes per mm^3 at episode onset		Average infected cell lifespan at episode onset, min	
Measures	High	Low	High	Low
Mean	10,622	1,063	133	14
95% CI	(10,592, 10,653)	(1,059, 1,069)	(132, 134)	(14, 14)
Range	(5,741, 15,936)	(112, 2,241)	(61, 621)	(9, 25)

Table S4. Number of low-, medium-, and high-copy HSV-2 shedding episodes from 10 365-d model simulations using ten different patient-derived parameter sets assuming both continuous and daily sampling

Shedding frequency, %	$CD8^+$T-cell expansion events per year	Infected cells killed by $CD8^+$T cells, %	Daily sampling number/percent				Continuous sampling number/percent			
			High	Medium	Low	Total	High	Medium	Low	Total
13.8	10	97.2	3	7	7	17	3	7	24	34
			18%	41%	41%		9%	21%	70%	
11.9	8	98.1	3	5	8	16	3	5	25	33
			19%	31%	50%		9%	15%	76%	
9.3	8	96.8	4	5	4	13	6	3	17	26
			31%	38%	31%		23%	12%	65%	
14.0	11	95.2	2	9	5	16	2	9	26	37
			13%	56%	31%		5%	24%	71%	
12.3	6	94.2	5	1	7	13	5	1	17	23
			38%	8%	54%		22%	4%	74%	
19.0	13	98.1	4	9	6	19	5	8	32	45
			21%	47%	32%		11%	18%	71%	
27.7	14	98.8	4	10	6	20	5	9	37	51
			20%	50%	30%		10%	18%	73%	
13.4	18	98.0	0	5	20	25	1	4	39	44
			0%	20%	80%		2%	9%	89%	
25.6	16	95.8	4	8	11	23	5	7	41	53
			17%	34%	49%		9%	13%	78%	
11.4	8	94.6	5	4	5	14	5	4	21	30
			36%	28%	36%		17%	13%	70%	

Low-, medium-, and high-copy episodes are defined as having a peak HSV-2 DNA copy number 10^2–10^4/mL, 10^4–10^6/mL, and $>10^6$/mL, respectively.

Table S5. Sensitivity analysis: Basic reproductive number, shedding frequency, episode frequency and recurrence frequency from 365-d model simulations using 20% adjustments in each parameter value

Parameter adjustments	R_0	Shedding frequency, %	Episodes				Recurrence frequency
			High	Medium	Low	Total	
Baseline	37.7	16.4	5	7	38	50	5
$CD8^+$ expansion rate = 1.2/d	37.7	16.7	5	8	30	43	4
$CD8^+$ expansion rate = 1.8/d	37.7	14.9	3	8	30	41	4
$CD8^+$ killing rate = 0.008 infected cells per $CD8^+$ per day	37.7	15.1	6	6	33	45	3
$CD8^+$ killing rate = 0.012 infected cells per $CD8^+$ per day	37.7	17.6	2	12	29	43	2
High infectivity = 1 infected cell per 16 HSV copies per day	43.4	17.6	5	8	38	51	5
Low infectivity = 1 infected cell per 20 HSV copies per day	34.7	11.2	4	6	31	41	4
Low burst phase = 8,000 HSV DNA copies per day	30.1	23.3	4	10	31	45	1
High burst phase = 12,000 HSV DNA copies per day	45.2	17.2	7	6	31	44	3
High viral lifespan = 2.5 h	47.1	20.2	4	8	30	42	4
Low viral lifespan = 1.7 h	32.0	17.6	4	10	25	39	2
Neuronal release rate = 25 HSV copies per day	37.7	11.2	4	6	16	26	3
Neuronal release rate = 100 HSV copies per day	37.7	22.3	3	11	45	59	3

For baseline measures, the following population parameter values were used to solve the model: infectivity: $\beta = 10^{-8}$/d; viral infectivity duration: $1/c = 2$ h; burst phase: $p = 10{,}000$ HSV DNA copies per infected cell per day; infected cell lifespan: $1/a = 20$ h; rate of HSV DNA released from neurons: $\phi = 50$ HSV DNA copies per day; rate of $CD8^+$ lymphocyte expansion: $\theta = 1.5$/d; Rate of clearance of infected cells by $CD8^+$ lymphocytes: $f = 0.01$ infected cells per $CD8^+$ T cell per day; $CD8^+$ lymphocyte lifespan: $1/\delta = 20$ d; $CD8^+$ lymphocyte antigen recognition: $r = 200$ infected cells needed before θ is half-maximal.

Table S6. Stochastic mathematical model of HSV-2 pathogenesis with assumption of $CD8^+$ trafficking from external sources rather than local replication within genital skin

Stochastic model equations*	Variables (starting values)	New parameters (values)
• $\Delta S = (\lambda - (\beta \times S \times V)) \Delta t$ • $\Delta I = ((\beta \times S \times V) - (a \times I) - (f \times I \times E)) \Delta t$ • $\Delta E = ((F(I)_I \times \theta_I) - (\delta \times E)) \Delta t$ • $F(I)_I = I/(I + r_i)$ • $\Delta Z = ((p \times I) - (c \times Z) - (\beta \times S \times Z)) \Delta t$ • $\Delta Y = (\phi - (c \times Y) - (\beta \times S \times Y)) \Delta t$ • $\lambda = d(S_0 - S)$ • $V = Z + Y$ • Δt = 1.5 min	• S = susceptible epidermal cells (5.42e6) • I = infected epidermal cells (zero) • E = $CD8^+$ lymphocytes (6,000, average value from a prior 365-d simulation) • Z = HSV DNA copy produced by an epidermal cell (zero) • Y = HSV DNA copy produced by neurons (zero)	• θ_I = $CD8^+$ T-cell infusion rate (3,000/d) • r_I = no. of infected cells before half-maximal $CD8^+$ T-cell infusion rate (2,000 infected cells)

*New model assumption: $CD8^+$ T cells replenish according to infected cell density only, rather than $CD8^+$ T-cell density in the presence of infected cells as in the model described in Table S1.